JCTC Journal of Chemical Theory and Computation

Article

pubs.acs.org/JCTC

# A Benchmark Ab Initio and DFT Study of the Structure and Binding of Methane in the σ−Alkane Complex $CpRe(CO)_2(CH_4)$

Bun Chan*,† and Graham E. Ball*,‡

†School of Chemistry and ARC Center of Excellence for Free Radical Chemistry and Biotechnology, University of Sydney, NSW 2006, Australia

‡School of Chemistry, University of New South Wales, NSW 2052, Australia

Supporting Information

**ABSTRACT:** Ab initio molecular orbital theory and density functional theory (DFT) procedures have been used to study the binding of methane in $CpRe(CO)_2(CH_4)$, the simplest σ−alkane complex in the experimentally widely studied $CpRe(CO)_2$(alkane) family. We find the optimal Re···C, Re···H and C···H distances to be 2.60, 1.92, and 1.15 Å, respectively, on the composite-CCSD(T)/def2-QZVPP (CCSD(T)/def2-TZVP with supplement for the larger def2-QZVPP basis set at the second-order Møller−Plesset perturbation theory level) potential energy surface which has been mapped out at this level of theory. The enthalpy of binding at 298 K was determined to be 62.0 kJ $mol^{-1}$ at the composite-CCSD(T)/CBS//B3-PW91/aug-cc-pVTZ-PP level. Benchmarks on the various DFT procedures show that some functionals give good geometries but underestimate binding energies, while others yield poor geometries but give closer agreements with the composite-CCSD(T) binding energy. On the other hand, the ωB97X-D functional gives fair agreements with composite-CCSD(T) for both geometry optimization as well as binding energy. Thus, it appears to be a reliable, easily implemented, and cost-effective means for studying Re−alkane complexes. Good binding energies are also obtained with several common functionals when D3 dispersion corrections are applied. Selected dispersion-corrected DFT methods (B3PW91-D3, TPSSh-D3, and B98-D3) were found to be quite accurate for the calculation of binding energies of several other model metal−$CH_4$ complexes containing a range of metal centers (Rh, Pd, W, Ir, Pt). We also note that, for single-point energy calculation of the Re−$CH_4$ binding, the PWP-B95-D3 double-hybrid DFT procedure provides an excellent agreement with the benchmark energy at only a slightly higher computational requirement.

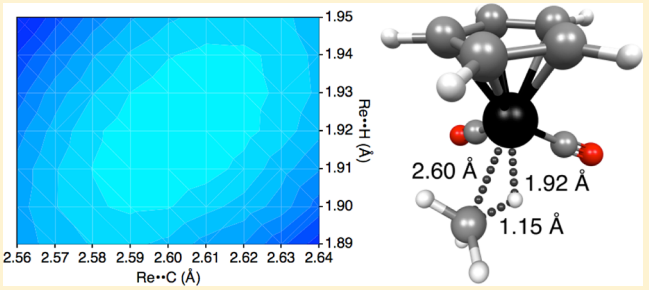


## INTRODUCTION

Transition-metal alkane σ-complexes have received significant attention in recent times using both experimental[1−3] and theoretical[4,5] approaches. The reason for the interest in these complexes is two-fold. First, they are of significant interest from the standpoint of fundamental coordination chemistry, held together by what is unsurprisingly a weak interaction.[6] Typically, they are considered to contain an essentially intact C−H σ-bond coordinated to a metal center, hence the term σ-complex, in what is termed an agostic interaction.[7−9] Second, and possibly even more important, they are frequently proposed to be key reactive intermediates in C−H activation reactions,[10,11] which constitute a useful step in the functionalization of hydrocarbon moieties,[12,13] sometimes even catalytically,[14−16] and other organometallic transformations such as the σ-complex assisted metathesis (σ-CAM) processes.[17] Primarily, alkane complexes have been observed using "fast" spectroscopic methods, such as time-resolved infrared (TRIR) spectroscopy, owing to the fact that alkane complexes are invariably short-lived in solution.[18] Occasionally alkane complexes have been isolated in the solid state and characterized crystallographically.[3,19,20]

One of the most well-studied classes of alkane σ-complexes are molecules of the type $CpRe(CO)_2$(alkane).[1] This class of molecules, such as $CpRe(CO)_2$(heptane), was first noted to be remarkably long-lived in comparison to other known alkane complexes.[21] The observation of the long lifetime facilitated the observation of the complexes using NMR spectroscopy.[22,23] Since then, several examples of $CpRe(CO)_2$(alkane)-type complexes have been observed using NMR spectroscopy,[24−27] and similar experimental observations have been made on compounds of the general type $LM(CO)_2$(alkane) (M = Re, L = Cp, Tp,[28] Kp;[29] Tp = hydrotris(pyrazol-1-yl)borate, Kp = cyclopentadienyltris(diethylphosphito)-cobaltate(III); M = Mn, L = Cp;[30] M = W, L = hexaethylbenzene, $C_6Et_6$).[31] Notably, most of the alkane complexes observed using NMR spectroscopy are resistant to cleavage, i.e., the C−H σ-complexes are apparently lower in energy than the alkyl hydride complexes that would result from cleavage of the C−H bond. In the case of the lightest alkane methane, however, a rapidly equilibrating mixture of the σ-

Received: January 4, 2013

   dx.doi.org/10.1021/ct400013p | J. Chem. Theory Comput. XXXX, XXX, XXX−XXX

complex isomer, $CpRe(CO)_2(CH_4)$ (**1**), and an oxidatively cleaved alkyl hydride isomer, $CpRe(CO)_2(CH_3)(H)$ (**2**), was observed using time-resolved infrared spectroscopy.[32] A lower limit of 51 ± 5 kJ mol$^{-1}$ for the binding enthalpy of the $CH_4$ in **1** was inferred from the activation barrier for the reaction of **1** with CO. In the case of the related heptane complex $CpRe(CO)_2$(heptane), activation parameters suggest a lower limit of 57.3 ± 0.9 kJ mol$^{-1}$ for the strength of the Re−heptane interaction.[33]

In addition to investigation by the various experimental techniques, theoretical/computational chemistry has been used to gain a deeper understanding of the fundamental interactions of these alkane complexes. Indeed the $CH_4$ complex (**1**) has been studied computationally previously. DFT methods (B3-LYP/SBK) were originally applied to the study of $CpRe(CO)_2(CH_4)$ (**1**) by Cundari et al.[34] They concluded that in this case the agostic interaction resulted in a noticeably large Re−H−C angle (118.9° calculated, internuclear distances calculated as Re−H, 1.99; Re−C, 2.73; C−H, 1.14). The binding energy of the methane was calculated to be 36 kJ mol$^{-1}$, and it was calculated that the alkane complex **1** and alkyl hydride **2** were close in energy in this case, with the alkyl hydride being higher in energy by only 3 kJ mol$^{-1}$.

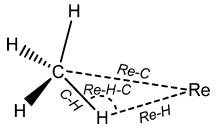


**Figure 1.** Diagram of the Re−$CH_4$ interaction in **1** showing key distances in italics.

In a later study, Head-Gordon and co-workers examined the binding of methane and numerous higher alkanes using DFT and second-order Møller−Plesset perturbation theory (MP2) methods[35] and performed a detailed analysis of the components of binding of the alkane to the rhenium fragment using the absolutely localized molecular orbital (ALMO) energy decomposition analysis method,[36] concluding that the most significant contribution to the bonding interaction was the charge transfer from the alkane to the metal fragment. A binding energy of 38 kJ mol$^{-1}$ was calculated at the B-P86/6-31G*,LANL2DZ level of theory, less than the experimental lower limit of 51 kJ mol$^{-1}$. The RI-MP2 calculations predicted a higher binding energy of 77 kJ mol$^{-1}$ (44 kJ mol$^{-1}$ when corrected for basis set superposition error).[35]

Other detailed computational studies of methane binding and activation include a study of the osmium complex $[(C_5Me_5)Os(Me_2PCH_2PMe_2)(CH_3)(H)]^+$ which undergoes exchange of alkyl and hydride hydrogens via the related methane complex $[(C_5Me_5)Os(Me_2PCH_2PMe_2)(CH_4)]^+$.[37] The performance of numerous different functionals at predicting geometric and energetic properties was evaluated and benchmarked against high-level coupled cluster calculations (CCSD(T)). They concluded that the use of dispersion-corrected functionals in conjunction with double-$\zeta$ or larger basis sets with polarization functions was recommended for calculations involving weak interactions, such as those found in transition-metal $\sigma$-complexes. The use of dispersion-corrected functionals and higher level wave function-based methods [local pair natural orbital (LPNO)-CCSD][38] has also been applied to rhenium and tungsten $\sigma$-complexes recently observed in our work.[29,31]

While some theoretical studies of $\sigma$-alkane complexes have occasionally utilized relatively accurate wave function procedures,[37,39,40] such as quadratic configuration interaction with single and double excitations (QCISD), CCSD, and CCSD(T), the relatively large size of these complexes with higher alkanes usually necessitates the use of more economical methods, typically DFT procedures. Although some contemporary DFT procedures have been shown to perform remarkably well for a wide range of chemical systems and properties, unlike for high-level wave function procedures, it remains risky to assume a general robustness for these methods. This is especially true when DFT procedures are applied to an entirely new class of systems that have not been previously tested. A commonly employed approach is therefore to apply a variety of different functionals to the problem leading to a range of results that are intended to bracket the correct values.

As DFT procedures are likely to remain the most cost-effective means for routine theoretical study of metal−alkane complexes, particularly with heavier alkanes, a thorough benchmark of their performance on these systems is of particular importance. To this end, in the present study, we use a prototypical metal−alkane complex, namely $CpRe(CO)_2(CH_4)$, to evaluate the reliability of a variety of DFT procedures for obtaining the geometry and binding energy. We have employed the high-level CCSD(T) procedure, together with large basis sets, to obtain reliable benchmark values. With these high-level theoretical computations, we also aim to gain further insights into the binding in $CpRe(CO)_2(CH_4)$ through mapping out the potential energy surface (PES) associated with the geometry of the key Re···H···C interaction which is shown to be relatively flat in this region. Functionals that give good agreement with the benchmark values for binding energies in the case of $CpRe(CO)_2(CH_4)$ were identified in this study. To test the general applicability of these methods, several of the most promising functionals were then tested on a range of methane complexes of different metals (Rh, Pd, W, Ir, Pt). The complexes surveyed represent model complexes for methane or heavier alkane complexes that either have been observed in the case of $[(PONOP^{tBu})Rh(CH_4)]^+$ ($PONOP^{tBu}$ = 2,6-($^tBu_2PO)_2C_5H_3N$; $^tBu$ = $C(CH_3)_3$)[2] and ($\eta^6$-hexaethylbenzene)$W(CO)_2$(pentane)[31] or have been considered as candidates for methane complex formation in the case of $[(PONOP)M(CH_4)]^{n+}$ (M = Ir, $n$ = 1; M = Pd, Pt, $n$ = 2).[5]

Overall, our results should allow more accurate prediction of the properties of larger $\sigma$-alkane complexes, such as $CpRe(CO)_2$(cyclohexane), which has previously been observed and studied computationally.[25] This will assist in studying the factors that influence alkane binding in systems of this genre and in identifying new target alkane complexes with stronger binding energies that may be stable in solution at or closer to ambient temperature.

## COMPUTATIONAL DETAILS

Standard ab initio molecular orbital theory and DFT calculations[41] were carried out with the Gaussian 09,[42] Molpro 2010,[43] and Orca 2.9[44] programs. An effective core potential (ECP) was applied to the transition-metal atom in all calculations. Basis sets and ECPs were obtained from the EMSL basis set exchange.[45] For geometry optimization, a number of basis sets were examined, namely def2-SVP, cc-pVDZ-PP (VDZ-PP), aug-cc-pVDZ-PP (AVDZ-PP), and aug-


dx.doi.org/10.1021/ct400013p | J. Chem. Theory Comput. XXXX, XXX, XXX−XXX

cc-pVTZ-PP (AVTZ-PP), in combination with a variety of 41 DFT procedures.

For single-point energy calculations, two types of composite scheme were employed in the present study. To obtain an approximate PES for the complex at a sufficiently high level of theory, we used the more economical protocol between the two schemes. This method approximates CCSD(T)/def2-QZVPP energies with the formula: composite-CCSD(T)/def2-QZVPP = CCSD(T)/def2-TZVP + MP2/def2-QZVPP − MP2/def2-TZVP. We refer to this composite-CCSD(T) scheme as C1-CCSD(T). To obtain a binding energy at the highest level that is currently reasonable, we use a more rigorous procedure. Thus, we obtain the complete basis set (CBS) limit at the MP2 level using the AVTZ-PP and AVQZ-PP basis sets, using the extrapolation formulas: $E_L = E_{CBS} + B \exp(-1.63\ L)$ for the Hartree−Fock component,[46,47] and $E_L = E_{CBS} + B\ L^{-3}$ for the MP2 correlation energy,[48] where $L$ is the cardinal number of the basis set, i.e., 3 for triple-$\zeta$ and 4 for quadruple-$\zeta$ basis sets. A correction for higher-order excitations: CCSD(T)/AVTZ-PP − MP2/AVTZ-PP, is then added to the MP2/CBS value to give the composite-CCSD(T)/CBS energy. We refer to this procedure as C2-CCSD(T).

To evaluate the performance of less computationally demanding methods, we have obtained single-point energies with the various DFT procedures using the def2-SVP, def2-TZVP, AVDZ-PP, and AVTZ-PP basis sets. Relative energies in benchmark comparisons are vibrationless values. Our best calculated binding enthalpy corresponds to C2-CCSD(T) 298 K enthalpy with the inclusion of contributions from zero-point vibrational energies (ZPVEs) and thermal corrections ($\Delta H_{vib}$), obtained using B3-PW91/AVTZ-PP harmonic vibrational frequencies scaled[49] by 0.9884 (ZPVE) and 0.9987 ($\Delta H_{vib}$).

## RESULTS AND DISCUSSION

**The Structure of $CpRe(CO)_2(CH_4)$.** We first examine the geometries of the $CpRe(CO)_2-CH_4$ complex obtained with the various DFT procedures and the effect of geometries on the C1-CCSD(T) (composite-CCSD(T)/def2-QZVPP) energies. Overall, there is only minor variation in the structure of the $CpRe(CO)_2$ fragment, with Re−CO distances of ∼1.90 Å, C≡O distances of ∼1.16 Å, and a distance of ∼1.94 Å between Re and the center of mass of the cyclopentadinenyl ring. On the other hand, there is a larger variation in the key interatomic distances between Re and $CH_4$, namely Re···C, Re···H, and C···H, in which the H atom corresponds to one that is closest to Re (Table 1). Overall, the variations lead to a wide range of the resulting C1-CCSD(T) energies (20 kJ mol$^{-1}$). Nonetheless, there are 62 methods that yield structures that are within 2 kJ mol$^{-1}$ of the lowest-energy structure, i.e., for the geometry obtained at the TPSSh/AVTZ-PP level (Table 2). Among these, there are 27 structures that fall in the range 0.0−1.5 kJ mol$^{-1}$, and 6 that are in the range 0.0−1.0 kJ mol$^{-1}$. Of the three key distances, we can see that the C···H distance only varies within a narrow range, with a range of only 0.004 Å for the standard deviation (SD) for the 27 lowest-energy structures that fall in the range 0.0−1.5 kJ mol$^{-1}$. There are much larger variations for the other two distances, with the larger variations found for Re···C (SD = 0.020 Å for the 27 lowest-energy structures). We have also examined the key bond lengths in the $CpRe(CO)_2$ fragment, and we find that their variations are also not as large as those in the Re···C and Re···H distances.

**Table 1. Number of Entries and SDs on Key Interatomic Distances (Å) between Re and $CH_4$ for Methods That Give Composite-CCSD(T)/def2-QZVPP Energies (kJ mol$^{-1}$) within Certain Ranges of the Lowest-Energy Structure**

| range | entries | Re···C | Re···H[a] | C···H[a] |
|---|---|---|---|---|
| 0.0−1.0 | 6 | 0.013 | 0.006 | 0.001 |
| 0.0−1.5 | 27 | 0.020 | 0.016 | 0.004 |
| 0.0−2.0 | 62 | 0.029 | 0.021 | 0.006 |
| 0.0−5.0 | 122 | 0.041 | 0.032 | 0.008 |
| 0.0−20.0 | 164 | 0.057 | 0.053 | 0.010 |

[a]H atom corresponds to one that is closest to Re.

While a large number of DFT procedures have yielded relatively low-energy structures, this by no means gives a solid indication on the structure of the complex. In particular, the Re···C and Re···H distances carry large uncertainties, as indicated by the relatively large SD values. We thus set out to refine the structure at the higher CCSD(T) level using a larger basis set. However, rather than carrying out an automated geometry optimization, the PES with respect to these three interatomic distances was examined in greater detail. As the geometry of the $CpRe(CO)_2$ fragment carries relatively small uncertainties, the refinement of the structure of the $Re-CH_4$ fragment alone is likely to be sufficient for a satisfactory description of the geometry of the complex. Thus the following procedure was employed in our refinement process: (1) We chose a geometry for the $CpRe(CO)_2$ fragment, obtained from the complex optimized with a relatively reliable DFT procedure, which is B3-PW91/AVTZ-PP in this case. (2) This was followed by optimizations at the B3-PW91/AVTZ-PP level with the following conditions: (a) atoms of the $CpRe(CO)_2$ moiety were fixed; (b) Re···C distance was scanned through 2.56−2.64 Å with intervals of 0.01 Å; and (c) Re···H distance was scanned through 1.89−1.95 Å with intervals of 0.01 Å. (3) Single-point energies at the C1-CCSD(T) level were calculated for each of the structures obtained by the constrained optimizations, and the lowest energy structure was determined.

Before we discuss the refined structure for the complex, it is appropriate to detail how the conditions in the refinement process were chosen. Table 2 shows the C1-CCSD(T) energies for the geometries fully optimized with the various DFT procedures, and the key bond distances between Re and $CH_4$, for which the C1-CCSD(T) energies are within 1.5 kJ mol$^{-1}$ of the lowest-energy structure. It also shows the average of the three key interatomic distances in the $Re-CH_4$ fragment, and the mean-absolute deviations (MADs) from the average values. In addition, because we set out to choose a geometry for the $CpRe(CO)_2$ fragment, we have examined the MADs for the key interatomic distances in this moiety and in the full $CpRe(CO)_2(CH_4)$ complex.

The choice to use the B3-PW91/AVTZ-PP geometry for the $CpRe(CO)_2$ fragment is based on energy, structural, and theoretical considerations, namely: (1) It has a relative C1-CCSD(T) energy that is at the lower end of the range, i.e., within 1 kJ mol$^{-1}$ of the lowest-energy structure; (2) it has the lowest MAD for the entire $CpRe(CO)_2(CH_4)$ complex of those within 1 kJ mol$^{-1}$ of the lowest energy structure; (3) in general, B3-PW91 has been shown to be a reasonably robust method for a wide-range of chemical systems, including heavy (second and third series) transition metals;[50] and (4) the large AVTZ-PP basis set is employed, which we deem somewhat more reliable than the double-$\zeta$ basis sets. Nonetheless, we


dx.doi.org/10.1021/ct400013p | J. Chem. Theory Comput. XXXX, XXX, XXX−XXX

Table 2. Relative Composite-CCSD(T)/def2-QZVPP Energies (kJ mol$^{-1}$), Key Interatomic Distances (Å), and MADs (Å) Relative to Average Distances in Various Fragments, for Various Geometries with Lowest Relative Energies (0.0−1.5 kJ mol$^{-1}$)

| DFT | basis set | energy | Re···C | Re···H | C···H | MAD (Re−$CH_4$) | MAD [CpRe $(CO)_2$] | MAD [CpRe $(CO)_2(CH_4)$] |
|---|---|---|---|---|---|---|---|---|
| TPSSh | AVTZ-PP | 0.00 | 2.614 | 1.926 | 1.146 | 0.0052 | 0.0057 | 0.0056 |
| $\tau$-HCTHhyb | AVTZ-PP | 0.12 | 2.626 | 1.927 | 1.147 | 0.0095 | 0.0030 | 0.0042 |
| B97-1 | AVTZ-PP | 0.14 | 2.628 | 1.932 | 1.147 | 0.0114 | 0.0058 | 0.0068 |
| B98 | AVTZ-PP | 0.41 | 2.631 | 1.928 | 1.146 | 0.0114 | 0.0067 | 0.0075 |
| CAM-B3-LYP | AVDZ-PP | 0.62 | 2.612 | 1.923 | 1.146 | 0.0055 | 0.0038 | 0.0041 |
| B3-PW91 | AVTZ-PP | 0.85 | 2.597 | 1.915 | 1.148 | 0.0055 | 0.0035 | 0.0039 |
| B97-2 | AVDZ-PP | 1.12 | 2.612 | 1.926 | 1.148 | 0.0036 | 0.0037 | 0.0037 |
| mPW3-PBE | AVTZ-PP | 1.14 | 2.583 | 1.909 | 1.150 | 0.0124 | 0.0048 | 0.0061 |
| mPW1-PW91 | def2-SVP | 1.16 | 2.603 | 1.937 | 1.148 | 0.0045 | 0.0041 | 0.0042 |
| CAM-B3-LYP | VDZ-PP | 1.18 | 2.628 | 1.929 | 1.147 | 0.0104 | 0.0044 | 0.0055 |
| HSE2-PBE | def2-SVP | 1.24 | 2.607 | 1.945 | 1.146 | 0.0091 | 0.0045 | 0.0053 |
| mPW1-PBE | def2-SVP | 1.29 | 2.594 | 1.932 | 1.150 | 0.0048 | 0.0031 | 0.0034 |
| B3-P86 | def2-SVP | 1.33 | 2.604 | 1.935 | 1.148 | 0.0041 | 0.0052 | 0.0050 |
| $\omega$B97X-D | AVDZ-PP | 1.34 | 2.601 | 1.923 | 1.150 | 0.0018 | 0.0047 | 0.0042 |
| HSE2-PBE | AVDZ-PP | 1.35 | 2.572 | 1.911 | 1.153 | 0.0160 | 0.0042 | 0.0063 |
| B97-2 | VDZ-PP | 1.37 | 2.629 | 1.933 | 1.148 | 0.0118 | 0.0035 | 0.0049 |
| $\omega$B97X | AVDZ-PP | 1.37 | 2.626 | 1.947 | 1.143 | 0.0170 | 0.0043 | 0.0065 |
| B3-PW91 | AVDZ-PP | 1.38 | 2.582 | 1.909 | 1.156 | 0.0143 | 0.0032 | 0.0051 |
| mPW1-PW91 | AVDZ-PP | 1.40 | 2.568 | 1.902 | 1.155 | 0.0214 | 0.0042 | 0.0073 |
| B3-P86 | AVTZ-PP | 1.43 | 2.585 | 1.908 | 1.147 | 0.0120 | 0.0052 | 0.0064 |
| HSEh1-PBE | AVTZ-PP | 1.45 | 2.584 | 1.915 | 1.147 | 0.0099 | 0.0062 | 0.0068 |
| PBEh1-PBE | def2-SVP | 1.46 | 2.603 | 1.944 | 1.148 | 0.0066 | 0.0041 | 0.0045 |
| HSEh1-PBE | AVDZ-PP | 1.46 | 2.571 | 1.911 | 1.155 | 0.0173 | 0.0042 | 0.0065 |
| HSEh1-PBE | def2-SVP | 1.46 | 2.606 | 1.945 | 1.148 | 0.0081 | 0.0045 | 0.0051 |
| HSE2-PBE | VDZ-PP | 1.47 | 2.588 | 1.917 | 1.152 | 0.0089 | 0.0038 | 0.0047 |
| M06 | AVDZ-PP | 1.48 | 2.617 | 1.969 | 1.141 | 0.0219 | 0.0027 | 0.0061 |
| B3-P86 | AVDZ-PP | 1.48 | 2.570 | 1.902 | 1.155 | 0.0205 | 0.0034 | 0.0064 |
| average | | | 2.602 | 1.926 | 1.149 | | | |

once again emphasize that most of the methods in Table 2 give very similar structures for the CpRe$(CO)_2$ fragment. Therefore, we do not expect a substantially different outcome if a slightly different geometry is chosen. The choice of the range for the Re···C and Re···H distances to scan is based on their average values (Table 2) and their uncertainties (Table 1, 0.0−1.5 kJ mol$^{-1}$). We have included two SDs for each interatomic distances to account for 95% confidence intervals, giving the respective values for Re···C and Re···H of 2.60 ± 0.04 and 1.92 ± 0.03 Å, i.e., with ranges of 2.56−2.64 and 1.89−1.95 Å, respectively.

We now examine the PESs obtained at the various levels from our constrained scan procedure (Figure 2). Compared with the B3-PW91/AVTZ-PP structure (Figure 2a), we can see that MP2 with both def2-TZVP and def2-QZVPP (Figure 2b,c, respectively) basis sets yields Re···C and Re···H distances that are substantially shorter. While we do not find a minimum on both MP2 surfaces, a comparison of the two contoured plots shows that MP2/def2-QZVPP has a slight tendency to give shorter distances. On the PES at the CCSD(T)/def2-TZVP level (Figure 2d), we find that the Re···C and Re···H distances are both longer than those at the B3-PW91/AVTZ-PP minimum. However, after adjusting for the basis set effect at the MP2 level, the C1-CCSD(T) (Figure 2e) and B3-PW91 minima lie very close to one another.

The procedure of the constrained scan yields an optimal Re···C distance of 2.60 Å. The Re···H distance in this structure is 1.92 Å, and the corresponding C···H distance is 1.15 Å (Figure 3). The corresponding Re···C, Re···H, and C···H distances at the B3-PW91/AVTZ-PP level are 2.597, 1.915, and 1.148 Å, respectively (Table 2). Using the B-P86 functional in combination with the 6-31G(d) and LANL2DZ basis sets, Cobar et al. have obtained the Re···C, Re···H, and C···H distances of 2.667, 1.970, and 1.155 Å, respectively.[35] Thus, while the C···H distance obtained in the previous study is comparable to our C1-CCSD(T) value, the Re···C and Re···H distances that we obtained are noticeably shorter.

We have also examined the B3-PW91/AVTZ-PP-optimized C···H distance as a function of the Re···C and Re···H distances (Figure 4). It is interesting to see that the C···H distance is relatively insensitive to the Re···C distance but increases as the Re···H distance shortens. The lengthening of the C−H bond is mainly governed by the donation of electron density from the C−H bonding orbital to the Re center, as revealed by a natural bond orbital[51] analysis at the B3-PW91/AVTZ-PP level, which shows an occupancy of 1.76 for the C−H bonding orbital, and strong donor−acceptor interactions from the C−H $\sigma$-orbital to several formally vacant re-centered orbitals.

**Assessment of DFT Procedures.** We now reassess the performance of the various DFT procedures for obtaining reliable geometries against the optimal C1-CCSD(T) values. Selected results for the methods listed in Table 2 are shown in Table 3, while the full results for all methods are given in Supporting Information. It is apparent that many DFT procedures give distances that are in close agreement with C1-CCSD(T). In fact, for the methods listed in Table 3, almost all yield MAD values that are smaller than 0.02 Å except M06/AVDZ-PP. Among all 164 methods examined, 67 have MADs that are smaller than 0.02 Å. For the cases in Table 3, 24 procedures out of 27 produce largest deviations (LDs) in which


dx.doi.org/10.1021/ct400013p | J. Chem. Theory Comput. XXXX, XXX, XXX−XXX

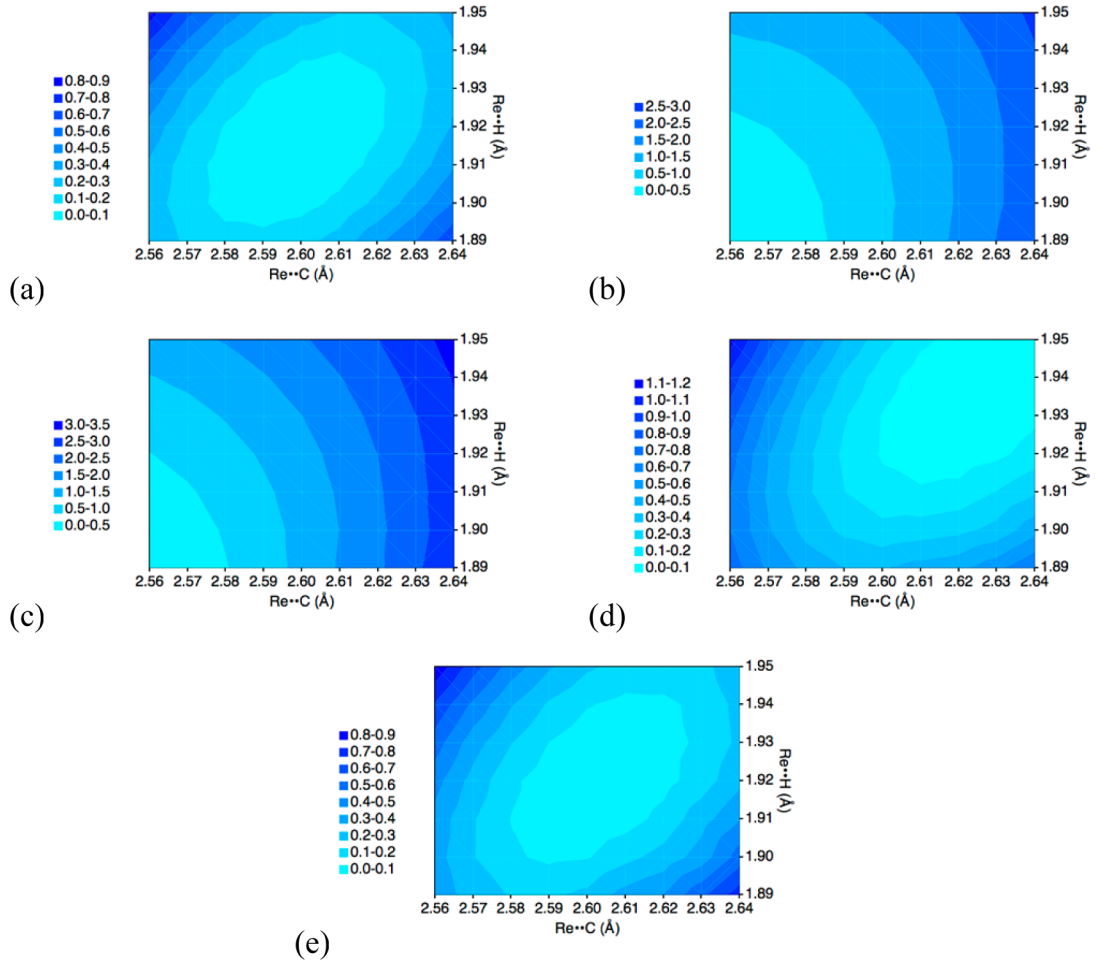


**Figure 2.** PESs as functions of the Re···C and Re···H distances (Å) at the various levels of theory: (a) B3-PW91/AVTZ-PP; (b) MP2/def2-TZVP; (c) MP2/def2-QZVPP; (d) CCSD(T)/def2-TZVP; and (e) composite-CCSD(T)/def2-QZVPP (C1-CCSD(T), in which the $CpRe(CO)_2$ fragment is held fixed at the B3-PW91/AVTZ-PP geometry.

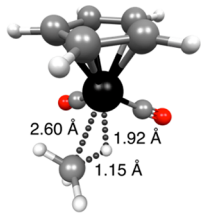


**Figure 3.** Minimum energy structure for constrained scan of Re···C and Re···H distances in the $CpRe(CO)_2(CH_4)$ complex at the composite-CCSD(T)/def2-QZVPP level.

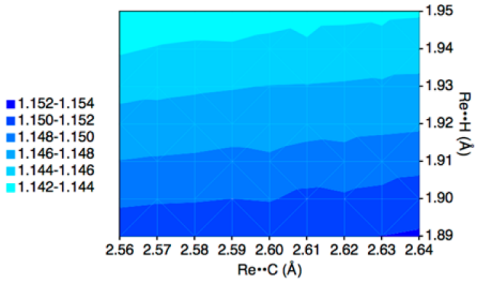


**Figure 4.** B3-PW91/AVTZ-PP optimized C···H distance (Å) as a function of the Re···C and Re···H distances.

the magnitudes are below 0.03 Å, and 13 in which the magnitudes of the LDs are no larger than 0.02 Å. While these 13 methods all give good agreements with the C1-CCSD(T) values, we find that B3-PW91 with the AVTZ-PP basis set and ωB97X-D/AVDZ-PP yield the best agreements for the three key interatomic distances. We also note that B3-PW91, when used in combination with the AVDZ-PP basis set, also gives a respectable geometry. This to some extent illustrates the robustness of this functional for geometry optimization for this complex.

In terms of how the choice of basis set affects the geometries, it can be seen that on going from the AVDZ-PP basis set to the larger AVTZ-PP basis from the same family, there is a systematic change in the key interatomic distances when the same functional is used, with the C−H distance increasing for all functionals by 0.009 Å on average and the Re−C and Re−H distances decreasing in all but one case (for Re−H) by an average amount of 0.018 and 0.008 Å, respectively. This is consistent with the smaller spatial span of the AVDZ-PP basis set drawing the $CpRe(CO)_2$ and $CH_4$ moieties closer together in the complex.

We note that the MD values for most DFT procedures are positive, both for the methods in Table 3 as well as for all 164 procedures. Thus, they tend to overestimate the distances. A survey of the three distances examined shows that the most significant deviations are for the Re···C and Re···H distances,


dx.doi.org/10.1021/ct400013p | J. Chem. Theory Comput. XXXX, XXX, XXX−XXX

Table 3. Relative Composite-CCSD(T)/def2-QZVPP Energies (kJ mol$^{-1}$), MDs, MADs, and LDs for Re···C, Re···H, and C···H Distances (Å) Obtained with Various DFT Procedures, Compared with Composite-CCSD(T)/def2-QZVPP Rigid Scan Values

| method | basis | energy | MD | MAD | LD |
|---|---|---|---|---|---|
| TPSSh | AVTZ-PP | 0.00 | 0.006 | 0.008 | 0.014 |
| $\tau$-HCTHhyb | AVTZ-PP | 0.12 | 0.010 | 0.012 | 0.026 |
| B97-1 | AVTZ-PP | 0.14 | 0.012 | 0.014 | 0.028 |
| B98 | AVTZ-PP | 0.41 | 0.012 | 0.014 | 0.031 |
| CAM-B3-LYP | AVDZ-PP | 0.62 | 0.004 | 0.007 | 0.012 |
| B3-PW91 | AVTZ-PP | 0.85 | −0.003 | 0.003 | −0.005 |
| B97-2 | AVDZ-PP | 1.12 | 0.005 | 0.007 | 0.012 |
| mPW3-PBE | AVTZ-PP | 1.14 | −0.010 | 0.010 | −0.017 |
| mPW1-PW91 | def2-SVP | 1.16 | 0.006 | 0.007 | 0.017 |
| CAM-B3-LYP | VDZ-PP | 1.18 | 0.011 | 0.013 | 0.028 |
| HSE2-PBE | def2-SVP | 1.24 | 0.009 | 0.012 | 0.025 |
| mPW1-PBE | def2-SVP | 1.29 | 0.002 | 0.006 | 0.012 |
| B3-P86 | def2-SVP | 1.33 | 0.006 | 0.007 | 0.015 |
| $\omega$B97X-D | AVDZ-PP | 1.34 | 0.001 | 0.001 | 0.003 |
| HSE2-PBE | AVDZ-PP | 1.35 | −0.011 | 0.013 | −0.028 |
| B97-2 | VDZ-PP | 1.37 | 0.013 | 0.015 | 0.029 |
| **$\omega$B97-X** | **AVDZ-PP** | **1.37** | **0.015** | **0.020** | **0.027** |
| B3-PW91 | AVDZ-PP | 1.38 | −0.007 | 0.011 | −0.018 |
| mPW1-PW91 | AVDZ-PP | 1.40 | −0.015 | 0.018 | −0.032 |
| B3-P86 | AVTZ-PP | 1.43 | −0.010 | 0.010 | −0.015 |
| HSEh1-PBE | AVTZ-PP | 1.45 | −0.008 | 0.008 | −0.016 |
| PBEh1-PBE | def2-SVP | 1.46 | 0.008 | 0.010 | 0.024 |
| HSEh1-PBE | AVDZ-PP | 1.46 | −0.011 | 0.014 | −0.029 |
| HSEh1-PBE | def2-SVP | 1.46 | 0.010 | 0.011 | 0.025 |
| HSE2-PBE | VDZ-PP | 1.47 | −0.004 | 0.006 | −0.012 |
| M06 | AVDZ-PP | 1.48 | 0.019 | 0.025 | 0.049 |
| B3-P86 | AVDZ-PP | 1.48 | −0.014 | 0.018 | −0.030 |

while the C···H distance tends to be mildly underestimated. We find that the VSXC pure functional produces the largest deviations among all DFT procedures examined, and it overestimates the Re···C and Re···H distances by at least 0.13 Å (with the AVDZ-PP basis set) and 0.21 Å (VDZ-PP), respectively. At the same time, it underestimates the C···H distance by at least 0.02 Å (VDZ-PP).

Turning our attention to the problem of obtaining reliable relative energies, we aim to identify DFT procedures that compare favorably with our benchmark C2-CCSD(T) (composite-CCSD(T)/CBS) method. Thus, we have calculated the complexation energies obtained with the various DFT procedures, using B3-PW91/AVTZ-PP-optimized geometries. We have also included two recently proposed double-hybrid DFT (DH-DFT) procedures, namely DuT[52] and PWP-B95,[53] in our comparison. These DH-DFT methods have been shown to yield adequate relative energies for a diverse set of thermochemical properties when used in conjunction with reasonably sized triple-$\zeta$-type basis sets. The complexation energies and corresponding deviations from the C2-CCSD(T) value of 65.9 kJ mol$^{-1}$ (corresponds to an enthalpy of 62.0 kJ mol$^{-1}$ at 298 K) are shown in Table 5.

For comparison, we have also obtained binding energies with a number of wave function procedures (Table 4). Very briefly, we note that MP2-type procedures severely overestimate the binding energies, while CCSD(T)-type methods, not surprisingly, yield values that are quite close to that obtained with the benchmark C2-CCSD(T) procedure. For both MP2- and

Table 4. Calculated CpRe(CO)$_2$(CH$_4$) Binding Energy (kJ mol$^{-1}$) Obtained Using Different Wavefunction Procedures with a Variety of Basis Sets

| method | basis set | binding energy | binding energy (with CP)[a] |
|---|---|---|---|
| MP2 | aug-cc-pVTZ-PP | 92.6 | 84.9 |
| MP2 | aug-cc-pVQZ-PP | 90.8 | |
| MP2 | def2-TZVP | 82.7 | |
| MP2 | def2-QZVPP | 88.0 | |
| MP2-F12 | def2-TZVP | 87.0 | |
| MP2-F12 | def2-QZVPP | 87.0 | |
| LCCSD(T) | aug-cc-pVTZ-PP | 68.9 | |
| CCSD(T) | aug-cc-pVTZ-PP | 68.6 | 61.6 |
| CCSD(T) | def2-TZVP | 59.2 | |
| CCSD(T)-F12b | def2-TZVP | 62.5 | |
| composite-CCSD(T)/def2-QZVPP | | 64.6 | |
| **composite-CCSD(T)/CBS** | | **65.9** | |

[a]Binding energy with the inclusion of counterpoise correction for basis set superposition error.

CCSD(T)-type procedures, the aug-cc-pVnZ-PP values converge from above, while def2-nZVP values converge from below, to the respective CBS limit. We also note that the use of explicitly correlated methods, namely, MP2-F12 and CCSD(T)-F12b, greatly accelerates the basis set convergence. We note, however, that the def2-TZVP basis set used in the F12 calculations are not designed to be used in the explicitly correlated calculations. Finally we note that the local LCCSD(T) method differs by a negligible amount (0.3 kJ mol$^{-1}$) from the analogous CCSD(T) method, and so local methods may provide a way to access highly accurate values on larger systems in the future.

We now return our attention to the performance of the DFT procedures. It is clear that most conventional functionals underestimate the binding between Re and CH$_4$, by as much as 54.7 kJ mol$^{-1}$ in the case of HCTH93/def2-TZVP. On the other hand, the BHandH procedure significantly overestimates the binding energy by more than 20 kJ mol$^{-1}$. In general, the use of the larger AVTZ-PP and def2-TZVP basis sets leads to binding energies that are smaller than those for the AVDZ-PP and def2-SVP basis sets, by an average of ∼4−6 kJ mol$^{-1}$, which is consistent with the presence of a somewhat larger basis set superposition error with the double-$\zeta$-type basis sets. Interestingly, while VSXC gives a poor structure for CpRe(CO)$_2$(CH$_4$) when it is used for geometry optimization, the VSXC//B3-PW91 complexation energies, perhaps fortuitously, agree reasonably well with the C2-CCSD(T) value. In contrast, B3-PW91 underestimates the binding energy by up to 20.6 kJ mol$^{-1}$. We find that five conventional functionals, when used with all the basis sets examined, give binding energies that are within ±10 kJ mol$^{-1}$ of the benchmark value. These are VSXC, LC-B-LYP, $\omega$B97X-D, LC-$\omega$PBE, and $\omega$B97.

Dispersion corrections compensate for the typical underestimation of the binding energy by conventional DFT procedures. Both the D3[54] and D3BJ[55,56] forms of dispersion corrections employed in the present study were designed for quadruple-$\zeta$ basis sets. Therefore, it can be expected that they are better suited to complement binding energies obtained with


dx.doi.org/10.1021/ct400013p | J. Chem. Theory Comput. XXXX, XXX, XXX−XXX

triple-ζ basis sets than the double-ζ values, and we consider only the results from triple-ζ basis sets here. For the 10 functionals for which both D3 and D3BJ corrections were evaluated, the average values of the binding energy were 61.7 and 65.4 kJ mol$^{-1}$, respectively, when the def2-TZVP basis set was employed and 45.8 kJ mol$^{-1}$ when no dispersion correction was applied. Hence, on average, the calculated binding energies are significantly closer to the benchmark value of 65.9 kJ mol$^{-1}$ when the dispersion corrections are included. A similar improvement is obtained with the larger AVTZ-PP basis, with the corresponding average values of the D3 and D3BJ binding energies being 64.8 and 68.5 kJ mol$^{-1}$, respectively, and 48.9 kJ mol$^{-1}$ when no dispersion correction was applied. Overall, with the use of the def2-TZVP basis set and after the inclusion of the D3 correction, we find that the dispersion-corrected procedures PBE1-PBE-D3, B1-B95-D3, TPSSh-D3, B3-PW91-D3, and B98-D3 give good binding energies (<4 kJ mol$^{-1}$ difference) when compared with the C2-CCSD(T) benchmark. In the absence of a unique approach for the estimation of dispersion contributions in the binding, we note that the large fraction of dispersion correction already indicates the significance of this component in the binding of these weakly interacting complexes. Such an observation regarding dispersion is in accord with, for example, a previous finding for a different type of complexes.[57]

The two DH-DFT procedures, on their own, provide fairly good agreement with the C2-CCSD(T) binding energy. We note that the DuT procedure, interestingly, slightly overestimates the strength of the binding, and therefore the use of the D3 correction would add to rather than compensate for the deviation from the benchmark value. On the other hand, the use of a D3 correction for PWP-B95 leads to very good agreement with the C2-CCSD(T) value.

What do we learn from the above benchmarks? Can we make recommendations on the appropriate theoretical procedures for the study of Re−alkane complexes? Among the methods tested for both geometry optimization and single-point energy calculation, the B3-PW91 functional gives excellent geometry for the $CpRe(CO)_2(CH_4)$ complex but does not yield satisfactory binding energies. The VSXC procedure yields very poor geometry, but when it is used for single-point energy calculations on better geometries, it gives surprisingly good complexation energies. In our opinion, neither of these DFT procedures lends us confidence in their usage. A survey of Tables 3 and 5 shows that ωB97X-D gives both reasonable geometries and adequate binding energies and is easily implemented. If D3 corrections are implemented for single point energies, several commonly employed functionals are deemed suitable for both geometries and energies including B3-PW91-D3 and also TPSSh-D3 and B98-D3 when the AVTZ-PP basis set is employed for geometry optimization. We also note that, where computational resources permits, the use of the PWP-B95-D3 procedure provides an accurate means for quantitative evaluation of the binding energy and has the advantage over the conventional DFT procedures of being less dependent on the empirical dispersion correction.

**Further Assessment of Additional Methane Complexes With Different Metals.** Are the above recommendations applicable to a wider range of complexes, or they are restricted to the specific type of complexes with Re? We attempt to answer this question by assessing the performance of several DFT procedures that are found to perform well for $CpRe(CO)_2(CH_4)$, namely, ωB97X-D, B3-PW91-D3, TPSSh-D3, and B98-D3, for a wider range of complexes. These include $(\eta^6\text{-benzene})W(CO)_2(CH_4)$, $[(PONOP)Rh(CH_4)]^+$,

**Table 5. Deviations of DFT Vibrationless Complexation Energies for $CpRe(CO)_2(CH_4)$ from the Composite-CCSD(T)/CBS Value and Dispersion (D3 and D3BJ) Corrections to Complexation Energies (kJ mol$^{-1}$)[a,b]**

| | | | | | dispersion corrections to DFT[b] | |
|---|---|---|---|---|---|---|
| | AVDZ -PP | AVTZ -PP | def2 -SVP | def2 -TZVP | D3 | D3BJ |
| BHandH | +28.0 | +22.5 | +23.0 | +19.8 | | |
| M06-HF | +12.3 | +9.4 | +9.9 | +3.9 | +2.2 | |
| VSXC | +7.5 | +2.2 | +3.7 | −0.9 | | |
| LC-B-LYP | +6.7 | +0.5 | +1.5 | −2.2 | | |
| **ωB97X-D** | **+3.2** | **−2.7** | **−3.1** | **−5.4** | | |
| LC-ωPBE | −0.5 | −5.2 | −5.5 | −8.4 | +13.1 | +14.0 |
| ωB97 | −0.3 | −6.0 | −6.8 | −8.9 | | |
| ωB97-X | −1.7 | −7.6 | −8.1 | −10.4 | | |
| PBEh1-PBE | −2.8 | −8.2 | −8.1 | −11.1 | | |
| PBE1-PBE | −3.1 | −8.3 | −8.2 | −11.3 | +11.5 | +12.3 |
| HSEh1-PBE | −3.1 | −8.5 | −8.4 | −11.3 | | |
| HSE2-PBE | −3.3 | −8.7 | −8.8 | −11.6 | | |
| M06-2X | −4.8 | −10.2 | −9.5 | −13.8 | +1.1 | |
| M06 | −3.4 | −11.0 | −10.3 | −14.2 | +3.6 | |
| B3-P86 | −5.6 | −11.4 | −11.5 | −14.3 | | |
| mPW1-PBE | −6.6 | −11.9 | −11.8 | −14.9 | | |
| mPW3-PBE | −7.5 | −13.0 | −12.6 | −16.0 | | |
| mPW1-PW91 | −7.7 | −13.0 | −12.9 | −16.0 | | |
| B97-D | −7.3 | −13.6 | −12.5 | −16.1 | | |
| B1-B95 | −8.7 | −13.9 | −13.3 | −17.2 | +15.6 | +18.8 |
| TPSSh | −9.6 | −14.6 | −14.9 | −17.6 | +14.7 | +29.4 |
| CAM-B3-LYP | −9.3 | −15.8 | −14.5 | −18.6 | +12.4 | +12.5 |
| τ-HCTHhyb | −10.0 | −16.2 | −15.8 | −18.8 | | |
| B97-1 | −12.0 | −17.9 | −17.6 | −21.1 | | |
| BMK | −13.4 | −18.9 | −18.9 | −21.9 | +17.1 | +18.9 |
| B3-PW91 | −11.8 | −18.5 | −18.7 | −22.8 | +20.0 | +22.9 |
| M06-L | −13.8 | −19.8 | −19.4 | −22.9 | | |
| B98 | −12.2 | −19.2 | −18.5 | −22.9 | +23.0 | +27.5 |
| X3-LYP | −18.7 | −25.3 | −23.7 | −28.1 | | |
| BHandH-LYP | −19.8 | −25.8 | −25.3 | −28.4 | +14.2 | +17.9 |
| mPW1-LYP | −19.2 | −25.8 | −23.9 | −28.7 | | |
| B97-2 | −20.7 | −26.0 | −26.0 | −28.9 | | |
| B3-LYP | −22.2 | −28.9 | −27.4 | −31.6 | +17.8 | +21.8 |
| B1-LYP | −26.0 | −31.6 | −31.1 | −33.7 | | |
| τ-HCTH | −24.4 | −31.0 | −29.6 | −33.8 | | |
| B-LYP | −30.0 | −37.4 | −34.3 | −40.3 | | |
| HCTH147 | −32.0 | −37.6 | −36.4 | −40.3 | | |
| HCTH | −39.1 | −44.1 | −42.4 | −46.6 | | |
| HCTH407 | −39.1 | −44.1 | −42.4 | −46.6 | | |
| O3-LYP | −39.5 | −44.6 | −43.1 | −47.4 | | |
| HCTH93 | −46.6 | −51.9 | −51.1 | −54.7 | | |
| DuT[c] | | +1.1 | | | +3.4 | |
| **PWP-B95**[d] | | **−8.2** | | | **+6.6** | **+7.2** |
| composite-CCSD(T)/CBS | | 65.9 | | | | |

[a]The same B3-PW91/AVTZ-PP-optimized geometries were used for all DFT and double-hybrid DFT single-point energy calculations. [b]The D3 or D3BJ corrections should be added to the corresponding binding energies to obtain the dispersion-corrected binding energies. [c]The AVTZ-PP basis set is used according to the recommended definition of the DuT procedure. [d]The def2-TZVPP basis set is used.


dx.doi.org/10.1021/ct400013p | J. Chem. Theory Comput. XXXX, XXX, XXX−XXX

$(PONOP)Pd(CH_4)]^{2+}$, $(PONOP)Ir(CH_4)]^{+}$, and $(PONOP)Pt(CH_4)]^{2+}$, where PONOP is 2,6-$(PH_2O)_2C_5H_3N$ (2,6-bis(phosphinooxy)pyridine).

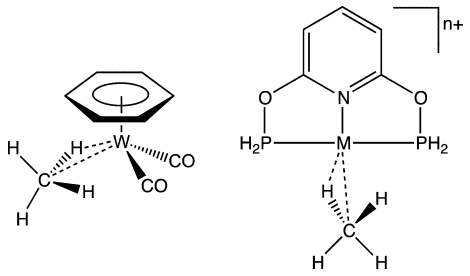


These complexes are closely related to the experimentally observed analogs,[2,5,31] with the direct coordination sphere and charge of the metal center being retained. The alkyl groups of the ligand have been replaced by hydrogens, and the heavier alkane replaced with methane in the case of the tungsten complex. These modifications facilitate the use of the CCSD(T) methods required for benchmarking. We employ the CCSD(T)-F12b/def2-TZVP procedure as a cost-effective means to obtain our benchmark binding energies. We note that, for $CpRe(CO)_2(CH_4)$, the deviation of the CCSD(T)-F12b binding energy from our highest C2-CCSD(T) level is only $-3.1$ kJ mol$^{-1}$ (Table 4). A comparison of the binding energies obtained with the DFT methods and those calculated with CCSD(T)-F12b is shown in Table 6.

We can see that, in all cases, $\omega$B97X-D/def2-TZVP somewhat underestimates the binding energies when compared with the CCSD(T)-F12b values, but the use of the AVTZ-PP basis set leads to an improved agreement with the benchmark. The B3-PW91, TPSSh, and B98 methods, by themselves, lead to more significant underestimation of the binding energies. However, the inclusion of the (original variant) D3 corrections leads to substantial improvement in the agreement with CCSD(T)-F12b values in all cases, with the resulting deviation being generally smaller than 5.1 kJ mol$^{-1}$. These observations are in accord with those for $CpRe(CO)_2(CH_4)$ and further supports the use of these DFT methods as a cost-effective means for the study of the binding between complexes of heavy transition metals and alkanes.

## CONCLUDING REMARKS

We have used ab initio and DFT procedures to study the binding energy for the $CpRe(CO)_2(CH_4)$ complex. Using a constrained scanning procedure, we have surveyed the PES for the Re···C and Re···H bonds at the composite-CCSD(T)/def2-QZVPP level and found the optimal Re···C, Re···H, and C···H distances to be 2.60, 1.92, and 1.15 Å, respectively. We have determined the 298 K binding enthalpy at the composite-CCSD(T)/CBS//B3-PW91/AVTZ-PP level to be 62.0 kJ mol$^{-1}$.

Regarding the reliability of the various DFT procedures, compared with the composite-CCSD(T) geometries and energies, we find that B3-PW91 gives a good geometry for the complex but does not yield reliable binding energies. On the other hand, VSXC gives a poor geometry, but when used for calculating binding energies on B3-PW91 structures, it leads to close agreements with the benchmark value. We do not recommend their usage in isolation for studying Re−alkane complexes due to such inconsistencies. On the other hand, $\omega$B97X-D gives reasonable agreements with composite-CCSD(T) for both geometry optimization as well as binding energy. In our opinion, it represents a reliable, cost-effective, and easily implemented means for studying complexation between Re and alkanes.

For the calculations of binding energies, we also note that most conventional DFT methods, as expected, yield underestimated values. This can be largely compensated for using the D3 dispersion correction scheme. The double-hybrid DFT procedure PWP-B95 gives moderate agreement with the benchmark binding energy without the D3 correction and excellent agreement when the dispersion correction is included. It thus appears to represent a robust means for the calculation of binding energy with a slightly higher computational requirement. For several of the best-performing conventional DFT procedures, namely, $\omega$B987X-D, B3-PW91-D3, TPSSh-D3, and B98-D3, we have further examined their performance for a wider range of metal−$CH_4$ complexes and find that they also yield binding energies that are quite accurate.

**Table 6. CCSD(T)-F12b and DFT Vibrationless Complexation Energies (kJ mol$^{-1}$) for the Different Metal−$CH_4$ Complexes and the Dispersion (D3 and D3BJ) Contributions to Complexation Energies (kJ mol$^{-1}$)[a−c]**

| ligands[d] | Cp $(CO)_2$ | PhH $(CO)_2$ | PONOP | PONOP | PONOP | PONOP |
|---|---|---|---|---|---|---|
| metal | Re | W | Rh | Pd | Ir | Pt |
| | | | Complexation Energies | | | |
| CCSD(T)-F12b | 62.4 | 49.8 | 85.2 | 115.7 | 103.5 | 143.3 |
| $\omega$B97X-D[e] | 60.4 (63.1) | 47.5 (49.2) | 77.2 (79.2) | 110.9 (113.8) | 97.5 (100.0) | 138.6 (142.1) |
| B3-PW91 | 44.0 | 31.4 | 67.3 | 99.0 | 88.2 | 128.1 |
| TPSSh | 48.3 | 37.0 | 72.5 | 103.0 | 92.0 | 131.5 |
| B98 | 43.0 | 31.8 | 64.0 | 96.4 | 83.6 | 124.2 |
| | | | Dispersion Corrections D3 (D3BJ) | | | |
| B3-PW91 | 20.0 (22.9) | 20.5 (24.2) | 14.6 (23.0) | 14.3 (21.9) | 15.8 (23.7) | 16.8 (23.8) |
| TPSSh | 14.7 (29.4) | 15.1 (30.7) | 10.6 (28.0) | 10.4 (25.1) | 11.4 (30.4) | 12.2 (29.6) |
| B98 | 23.0 (27.5) | 23.1 (28.6) | 18.7 (28.1) | 18.0 (26.9) | 20.3 (28.7) | 21.4 (28.9) |

[a]The same B3-PW91/AVTZ-PP-optimized geometries were used for all DFT single-point energy calculations. [b]The D3 or D3BJ corrections should be added to the corresponding binding energies to obtain the dispersion-corrected binding energies. [c]The def2-TZVP basis set is used for both CCSD(T)-F12b and DFT procedures. [d]Cp = cyclopentadienyl, PhH = benzene, PONOP = 2,6-$(PH_2O)_2C_5H_3N$ (2,6-bis(phosphinooxy)pyridine). [e]The AVTZ-PP values are shown in parentheses.


dx.doi.org/10.1021/ct400013p | J. Chem. Theory Comput. XXXX, XXX, XXX−XXX

## ■ ASSOCIATED CONTENT

### Supporting Information

B3-PW91/AVTZ-PP-optimized geometries for all complexes examined in the present study, selected interatomic distances for the $CpRe(CO)_2(CH_4)$ complex (Table S1), vibrationless electronic energies for all species, and the corresponding vibrationless binding energies (Table S2). This material is available free of charge via the Internet at http://pubs.acs.org.

## ■ AUTHOR INFORMATION


### Corresponding Authors

*E-mail: chan_b@chem.usyd.edu.au

*E-mail: g.ball@unsw.edu.au


### Notes

The authors declare no competing financial interest.

## ■ ACKNOWLEDGMENTS

We gratefully acknowledge funding from the Australian Research Council (DP0881692). This research was undertaken with the assistance of resources provided at the NCI National Facility, Canberra and INTERSECT which are supported by the Australian Government.

## ■ REFERENCES


(1) Cowan, A. J.; George, M. W. *Coord. Chem. Rev.* **2008**, *252*, 2504−2511.

(2) Bernskoetter, W. H.; Schauer, C. K.; Goldberg, K. I.; Brookhart, M. *Science (Washington, DC, U. S.)* **2009**, *326*, 553−556.

(3) Pike, S. D.; Thompson, A. L.; Algarra, A. G.; Apperley, D. C.; MacGregor, S. A.; Weller, A. S. *Science (Washington, DC, U.S.)* **2012**, *337*, 1648−1651.

(4) Balcells, D.; Clot, E.; Eisenstein, O. *Chem. Rev. (Washington, DC, U.S.)* **2010**, *110*, 749−823.

(5) Walter, M. D.; White, P. S.; Schauer, C. K.; Brookhart, M. *New J. Chem.* **2011**, *35*, 2884−2893.

(6) Hall, C.; Perutz, R. N. *Chem. Rev. (Washington, DC, U.S.)* **1996**, *96*, 3125−3146.

(7) Brookhart, M.; Green, M. L. H. *J. Organomet. Chem.* **1983**, *250*, 395−408.

(8) Brookhart, M.; Green, M. L. H.; Wong, L. L. *Prog. Inorg. Chem.* **1988**, *36*, 1−124.

(9) Brookhart, M.; Green, M. L. H.; Parkin, G. *Proc. Natl. Acad. Sci. U.S.A.* **2007**, *104*, 6908.

(10) Jones, W. D.; Vetter, A. J.; Wick, D. D.; Northcutt, T. O. *ACS Symp. Ser.* **2004**, *885*, 56−69.

(11) Lersch, M.; Tilset, M. *Chem. Rev. (Washington, DC, U.S.)* **2005**, *105*, 2471−2526.

(12) Labinger, J. A.; Bercaw, J. E. *Nature (London, U.K.)* **2002**, *417*, 507−514.

(13) Crabtree, R. H. *J. Organomet. Chem.* **2004**, *689*, 4083−4091.

(14) Mkhalid, I. A. I.; Barnard, J. H.; Marder, T. B.; Murphy, J. M.; Hartwig, J. F. *Chem. Rev. (Washington, DC, U.S.)* **2010**, *110*, 890−931.

(15) Conley, B. L.; Tenn, W. J.; Young, K. J. H.; Ganesh, S. K.; Meier, S. K.; Ziatdinov, V. R.; Mironov, O.; Oxgaard, J.; Gonzales, J.; Goddard, W. A.; Periana, R. A. *J. Mol. Catal. A: Chem.* **2006**, *251*, 8−23.

(16) Ahlquist, M.; Nielsen, R. J.; Periana, R. A.; Goddard, W. A., III *J. Am. Chem. Soc.* **2009**, *131*, 17110−17115.

(17) Perutz, R. N.; Sabo-Etienne, S. *Angew. Chem., Int. Ed.* **2007**, *46*, 2578−2592.

(18) Calladine, J. A.; Vuong, K. Q.; Sun, X. Z.; George, M. W. *Pure Appl. Chem.* **2009**, *81*, 1667−1675.

(19) Evans, D. R.; Drovetskaya, T.; Bau, R.; Reed, C. A.; Boyd, P. D. W. *J. Am. Chem. Soc.* **1997**, *119*, 3633−3634.

(20) Castro-Rodriguez, I.; Nakai, H.; Gantzel, P.; Zakharov, L. N.; Rheingold, A. L.; Meyer, K. *J. Am. Chem. Soc.* **2003**, *125*, 15734−15735.

(21) Sun, X.-Z.; Grills, D. C.; Nikiforov, S. M.; Poliakoff, M.; George, M. W. *J. Am. Chem. Soc.* **1997**, *119*, 7521−7525.

(22) Geftakis, S.; Ball, G. E. *J. Am. Chem. Soc.* **1999**, *121*, 6336−6336.

(23) Geftakis, S.; Ball, G. E. *J. Am. Chem. Soc.* **1998**, *120*, 9953−9954.

(24) Lawes, D. J.; Geftakis, S.; Ball, G. E. *J. Am. Chem. Soc.* **2005**, *127*, 4134−4135.

(25) Lawes, D. J.; Darwish, T. A.; Clark, T.; Harper, J. B.; Ball, G. E. *Angew. Chem., Int. Ed.* **2006**, *45*, 4486−4490.

(26) Calladine, J. A.; Torres, O.; Anstey, M.; Ball, G. E.; Bergman, R. G.; Curley, J.; Duckett, S. B.; George, M. W.; Gilson, A. I.; Lawes, D. J.; Perutz, R. N.; Sun, X.-Z.; Vollhardt, K. P. C. *Chem. Sci* **2010**, *1*, 622−630.

(27) Ball, G. E. *Spectrosc. Prop. Inorg. Organomet. Compd.* **2010**, *41*, 262−287.

(28) Duckett, S. B.; George, M. W.; Jina, O. S.; Matthews, S. L.; Perutz, R. N.; Sun, X.-Z.; Vuong, K. Q. *Chem. Commun. (Cambridge, U.K.)* **2009**, 1401−1403.

(29) Young, R. D.; Hill, A. F.; Hillier, W.; Ball, G. E. *J. Am. Chem. Soc.* **2011**, *133*, 13806−13809.

(30) Calladine, J. A.; Duckett, S. B.; George, M. W.; Matthews, S. L.; Perutz, R. N.; Torres, O.; Vuong, K. Q. *J. Am. Chem. Soc.* **2011**, *133*, 2303−2310.

(31) Young, R. D.; Lawes, D. J.; Hill, A. F.; Ball, G. E. *J. Am. Chem. Soc.* **2012**, *134*, 8294−8297.

(32) Cowan, A. J.; Poritus, P.; Kawanami, H. K.; Jina, O. S.; Grills, D. C.; Sun, X.-Z.; McMaster, J.; George, M. W. *Proc. Natl. Acad. Sci. U.S.A.* **2007**, *104*, 6933−6938.

(33) Bengali, A. A. *J. Organomet. Chem.* **2005**, *690*, 4989−4992.

(34) Bergman, R. G.; Cundari, T. R.; Gillespie, A. M.; Gunnoe, T. B.; Harman, W. D.; Klinckman, T. R.; Temple, M. D.; White, D. P. *Organometallics* **2003**, *22*, 2331−2337.

(35) Cobar, E. A.; Khaliullin, R. Z.; Bergman, R. G.; Head-Gordon, M. *Proc. Natl. Acad. Sci. U.S.A.* **2007**, *104*, 6963−6968.

(36) Khaliullin, R. Z.; Cobar, E. A.; Lochan, R. C.; Bell, A. T.; Head-Gordon, M. *J. Phys. Chem. A* **2007**, *111*, 8753−8765.

(37) Flener-Lovitt, C.; Woon, D. E.; Dunning, T. H.; Girolami, G. S. *J. Phys. Chem. A* **2010**, *114*, 1843−1851.

(38) Neese, F.; Hansen, A.; Liakos, D. G. *J. Chem. Phys.* **2009**, *131*, 064103/1−064103/20.

(39) Zaric, S.; Hall, M. B. *J. Phys. Chem. A* **1997**, *101*, 4646−4652.

(40) George, M. W.; Hall, M. B.; Jina, O. S.; Portius, P.; Sun, X.-Z.; Towrie, M.; Wu, H.; Yang, X.; Zaric, S. D. *Proc. Natl. Acad. Sci. U.S.A.* **2010**, *107*, 20178−20183.

(41) See, for example: (a) Hehre, W. J.; Radom, L.; Schleyer, P. v. P.; Pople, J. A. *Ab Initio Molecular Orbital Theory*; Wiley: New York, 1986. (b) Koch, W.; Holthausen, M. C. *A Chemist's Guide to Density Functional Theory*, 2nd ed.; Wiley: New York, 2001. (c) Jensen, F. *Introduction to Computational Chemistry*, 2nd ed.; Wiley: Chichester, 2007.

(42) Frisch, M. J.; Trucks, G. W.; Schlegel, H. B.; Scuseria, G. E.; Robb, M. A.; Cheeseman, J. R.; Scalmani, G.; Barone, V.; Mennucci, B.; Petersson, G. A.; Nakatsuji, H.; Caricato, M.; Li, X.; Hratchian, H. P.; Izmaylov, A. F.; Bloino, J.; Zheng, G.; Sonnenberg, J. L.; Hada, M.; Ehara, M.; Toyota, K.; Fukuda, R.; Hasegawa, J.; Ishida, M.; Nakajima, T.; Honda, Y.; Kitao, O.; Nakai, H.; Vreven, T.; Montgomery, J. A., Jr.; Peralta, J. E.; Ogliaro, F.; Bearpark, M.; Heyd, J. J.; Brothers, E.; Kudin, K. N.; Staroverov, V. N.; Kobayashi, R.; Normand, J.; Raghavachari, K.; Rendell, A.; Burant, J. C.; Iyengar, S. S.; Tomasi, J.; Cossi, M.; Rega, N.; Millam, N. J.; Klene, M.; Knox, J. E.; Cross, J. B.; Bakken, V.; Adamo, C.; Jaramillo, J.; Gomperts, R.; Stratmann, R. E.; Yazyev, O.; Austin, A. J.; Cammi, R.; Pomelli, C.; Ochterski, J. W.; Martin, R. L.; Morokuma, K.; Zakrzewski, V. G.; Voth, G. A.; Salvador, P.; Dannenberg, J. J.; Dapprich, S.; Daniels, A. D.; Farkas, Ö.; Foresman, J. B.; Ortiz, J. V.; Cioslowski, J.; Fox, D. J. *Gaussian 09*, revision A.02; Gaussian, Inc.: Wallingford, CT, 2009.

(43) Werner, H.-J.; Knowles, P. J.; Manby, F. R.; M. Schütz, Celani, P.; Knizia, G.; Korona, T.; Lindh, R.; Mitrushenkov, A.; Rauhut, G.; Adler, T. B.; Amos, R. D.; Bernhardsson, A.; Berning, A.; Cooper, D. L.; Deegan, M. J. O.; Dobbyn, A. J.; Eckert, F.; Goll, E.; Hampel, C.; Hesselmann, A.; Hetzer, G.; Hrenar, T.; Jansen, G.; C. Köppl, Liu, Y.; Lloyd, A. W.; Mata, R. A.; May, A. J.; McNicholas, S. J.; Meyer, W.; Mura, M. E.; Nicklaß, A.; Palmieri, P.; K. Pflüger, Pitzer, R.; Reiher, M.; Shiozaki, T.; Stoll, H.; Stone, A. J.; Tarroni, R.; Thorsteinsson, T.; Wang, M.; Wolf, A. *MOLPRO*; Cardiff University and University of Stuttgart: Cardiff, Wales and Stuttgart, Germany, 2012
(44) Neese, F. *Wiley Interdiscip. Rev. Comput. Mol. Sci.* **2012**, *2*, 73−78.
(45) Schuchardt, K. L.; Didier, B. T.; Elsethagen, T.; Sun, L.; Gurumoorthi, V.; Chase, J.; Li, J.; Windus, T. L. *J. Chem. Inf. Model.* **2007**, *47*, 1045−1052.
(46) Dunning, T. H., Jr. *J. Chem. Phys.* **1989**, *90*, 1007−1023.
(47) Feller, D.; Peterson, K. A. *J. Chem. Phys.* **1998**, *108*, 154−176.
(48) Halkier, A.; Helgaker, T.; Jorgensen, P.; Klopper, W.; Koch, H.; Olsen, J.; Wilson, A. K. *Chem. Phys. Lett.* **1998**, *286*, 243−252.
(49) Merrick, J. P.; Moran, D.; Radom, L. *J. Phys. Chem. A* **2007**, *111*, 11683−11700.
(50) For recent benchmark studies, see for example: (a) Tekarli, S. M.; Drummond, M. L.; Williams, T. G.; Cundari, T. R.; Wilson, A. K. *J. Phys. Chem. A* **2009**, *113*, 8607−8614. (b) Goerigk, L.; Grimme, S. *Phys. Chem. Chem. Phys.* **2011**, *13*, 6670−6688. (c) Buhl, M.; Reimann, C.; Pantazis, D. A.; Bredow, T.; Neese, F. *J. Chem. Theory Comput.* **2008**, *4*, 1449−1459.
(51) Glendening, E. D.; Landis, C. R.; Weinhold, F. *Wiley Interdiscip. Rev. Comput. Mol. Sci.* **2012**, *2*, 1−42.
(52) Chan, B.; Radom, L. *J. Chem. Theory Comput.* **2011**, *7*, 2852−2863.
(53) Goerigk, L.; Grimme, S. *J. Chem. Theory Comput.* **2011**, *7*, 291−309.
(54) Grimme, S.; Antony, J.; Ehrlich, S.; Krieg, H. *J. Chem. Phys.* **2010**, *132*, 154104/1−154104/19.
(55) Becke, A. D.; Johnson, E. R. *J. Chem. Phys.* **2005**, *123*, 154101/1−154101/9.
(56) Grimme, S.; Ehrlich, S.; Goerigk, L. *J. Comput. Chem.* **2011**, *32*, 1456−1465.
(57) Ryde, U.; Mata, R. A.; Grimme, S. *Dalton Trans.* **2011**, *40*, 11176−11183.